

Photon Transfer Methods and Results For Electron Multiplication CCDs

Michael J. DeWeert, Jeffrey B. Cole, Andrew W. Sparks, and Andrew Acker

BAE Systems Spectral Solutions, 999 Bishop Street Suite 2700, Honolulu, HI, 96813

ABSTRACT

Optical systems designed for some defense, environmental, and commercial remote-sensing applications must simultaneously have a high dynamic range, high sensitivity, and low noise-equivalent contrast. We have adapted James Janesick's photon transfer technique for characterizing the noise performance of an electron multiplication CCD (EMCCD), and we have developed methods for characterizing performance parameters in a lab environment. We have defined a new figure of merit to complement the traditionally used dynamic range that quantifies the usefulness of EMCCD imagers. We use the results for EMCCDs to predict their performance with hyperspectral and multispectral imaging systems.

Keywords:

Photon transfer, electron multiplication, CCD, remote sensing, hyperspectral, multispectral, noise equivalent contrast, NEC, dynamic range, noise factor.

1. INTRODUCTION

1.1. Overview

A significant recent advance in intensified imaging is provided by electron multiplication charge-coupled device (EMCCD) technology. These devices use a several-hundred-element readout register that can produce gains of several orders of magnitude. Because the gain at each stage is typically on the order of 1%, the excess noise factor is modest, amounting to a factor of approximately two.¹

BAE Systems Spectral Solutions LLC has evaluated the noise and gain characteristics of EMCCDs, with an eye toward their possible inclusion in sensor systems for commercial and defense use. This paper presents some results of these evaluations, including photon transfer, quantum efficiency (QE), and excess noise factor measurements. An EMCCD camera was tested to determine how it would function at low light levels (less than 100 photons per exposure) and to better understand the effects of electron multiplication gain (EMG). The tests were intended to measure noise characteristics, quantum efficiency, absolute photo-response, EMG relative to the video gain, noise equivalent contrast (NEC), and excess noise factor caused by EMG.

In addition, we have found that the extremely low read-noise floor of these devices requires a definition of system dynamic range that goes beyond traditional literature usage. To avoid confusion with the traditionally defined dynamic range, we propose to call this quantity the useable signal range (USR). This allows us to adapt Janesick's method² for EMCCDs in a manner that can be optimized for specific applications.

1.2. Definitions and Background

The notation and terms used in this paper are summarized in Table 1. Some of the terms are clarified in the diagram in Figure 1, which outlines the basic feature of EMCCD operation.

The camera used in our testing is an electron multiplication CCD (EMCCD) designed for low-light imaging on the order of single photons. During the EM gain stage, a voltage is applied to the signal electrons and the signal is amplified through impact ionization¹. The net response to an input photon flux is described by the schematic shown in Figure 1.

Table 1. Terms and Notations

Notation	Description	Units
ph	Photons	photons
$pe^-_{pre} = pe^-_{pre,Signal} + pe^-_{pre,Dark}$	Electrons entering the EMG stage	photo-electrons
$S^2_{pre,pe-}$	Variance of electrons entering the EMG stage	(photo-electrons) ²
pe^-_{post}	Electrons exiting the EMG stage	electrons
$S^2_{post,e-}$	Variance of electrons exiting the EMG stage	(electrons) ²
DN	Digital Numbers	DN
$S_{Total, DN}$	Total signal including bias offset	DN
$S_{Offset, DN}$	Signal bias offset	DN
S_{DN}	Signal (with bias subtracted)	DN
M	Multiplication Gain Ratio	-
A	Video Gain	DN / electron
G	Total system gain	DN / photo-electron
R_1	Absolute photo-response	DN / photon
QE_1	Quantum Efficiency (a function of wavelength)	photo-electron / photon
F	Noise Factor, defined as a Fraction of Variance	-
NEC	Noise Equivalent Contrast (noise / signal)	-
$S^2_{Total, DN}$	Total variance of signal	(DN) ²
$S^2_{DifferencedFrames, DN}$	Total variance of differenced frames	(DN) ²
$S^2_{Read, DN}$	Read noise of signal	(DN) ²
$S^2_{Shot, DN}$	Shot noise of signal	(DN) ²
$S^2_{FP, DN}$	Fixed pattern noise of signal	(DN) ²
$S^2_{ADC, DN}$	Digitization Noise from video gain	(DN) ²
$S^2_{Total, pe-}$	Total variance of signal	(photo-electrons) ²
$S^2_{Dark, e-}$	Dark noise of signal	electrons
$S^2_{Read, pe-}$	Read noise of signal	(photo-electrons) ²
$S^2_{Shot, pe-}$	Shot noise of signal	(photo-electrons) ²
$S^2_{FP, pe-}$	Fixed pattern noise of signal	(photo-electrons) ²
FW_{DN}	Pixel Full Well	DN
FW_{e-}	Pixel Full Well	electrons
DR	Dynamic Range	-
USR_{SNR}	Usable Signal Range between a signal at some specified SNR and the full well	-

The processes illustrated in Figure 1 result in the following relationship between input photons and output digitizer counts:

$$S_{DN} = R_I \times ph \quad (1)$$

When the photons arrive at the sensor some photons will be absorbed and converted into photoelectrons. This process is wavelength dependent and can be described by a scaling factor QE_1 :

$$QE_1 = \frac{pe^-_{pre}}{ph} \quad (2)$$

The photoelectrons are then passed through the EM gain stage where they are multiplied by a gain factor M :

$$M = \frac{pe^-_{post}}{pe^-_{pre}} \quad (3)$$

Finally, the photo-electrons leaving the EM gain stage are converted into a digital number at the analog-to-digital converter. This final gain stage is known as video gain and has a conversion factor A :

$$A = \frac{S_{DN}}{pe^-_{post}} \quad (4)$$

The overall system photo-response can be described by combining the three conversion stages:

$$R_I = QE_1 \cdot A \cdot M \quad (5)$$

The last two stages can be combined and considered as the total gain G :

$$G = M \cdot A \quad (6)$$

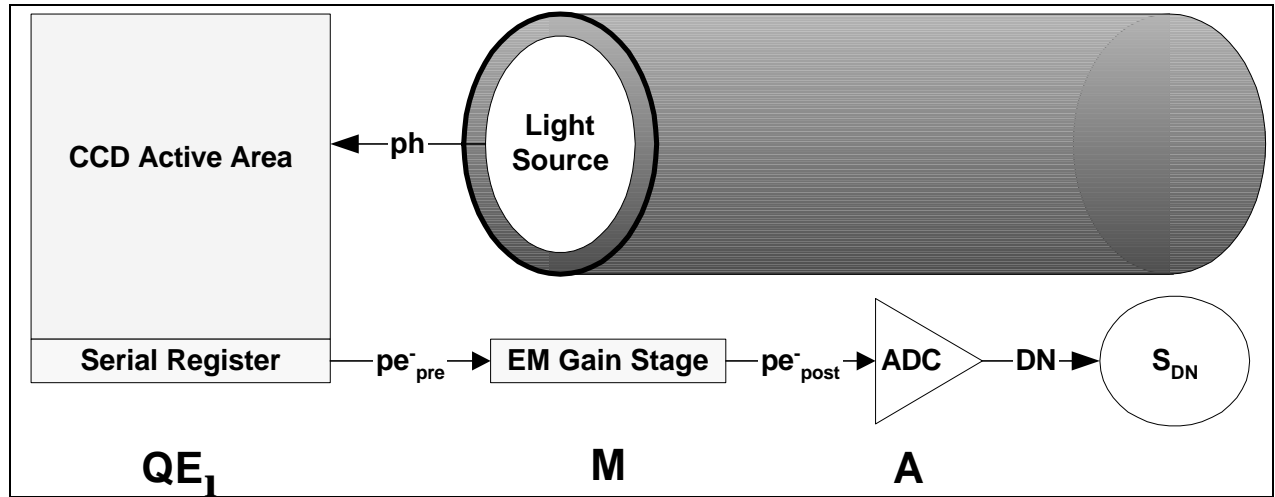


Figure 1. EMCCD function. An EMCCD operates exactly like a traditional CCD except that an additional gain stage is added between the serial register and the analog to digital converter.

The electron multiplication gain ratio, M , is controlled by varying the voltage applied to the EM gain stages. For the camera tested, a 12-bit slider is controlled through a software interface to set the electron multiplication gain. The gain ratio increases as the voltage-slider is turned up. When the slider is set to 0, the EM gain stage transfers the charge exactly like the serial register, which essentially eliminates the EM gain stage and makes M equal to unity (Figure 2).

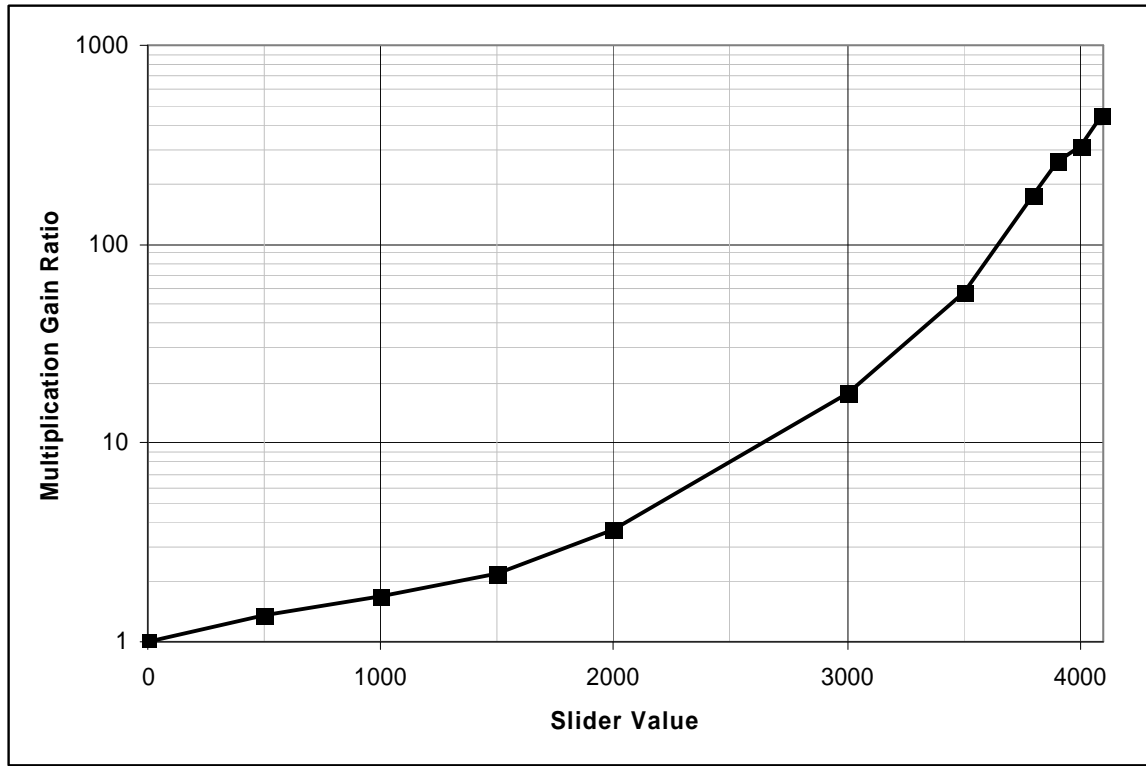


Figure 2. Measured EMG gain versus software-slider setting.

1.3. Noise in CCDs and EMCCDs

In EMCCDs, the primary EMG process occurs before the signal is converted into digital numbers. Throughout this paper, we use an additive noise model, summing variances for read, shot, dark, fixed-pattern and digitization noise sources:

$$\mathbf{s}_{Total,DN}^2 = \mathbf{s}_{Read,DN}^2 + \mathbf{s}_{Shot,DN}^2 + \mathbf{s}_{Dark,DN}^2 + \mathbf{s}_{FP,DN}^2 + \mathbf{s}_{ADC,DN}^2 \quad (7)$$

In terms of electrons and photo-electrons, this is:

$$\mathbf{s}_{Total,DN}^2 \approx A^2 \mathbf{s}_{Read,pe^-}^2 + G^2 F (pe_{Signal}^- + pe_{Dark}^-) + G^2 \mathbf{a}_{fp,DN} (pe_{Signal}^-)^2 + 1/12 \quad (8)$$

where F is the excess noise factor of the EMCCD, \mathbf{a}_{fp} is a constant characterizing the relative pixel-to-pixel response variability, and we have assumed Poisson statistics for the noise associated with the dark current. Note that F in Equation (8) is defined as a fractional increase in variance. We emphasize this because some authors [1] define noise factor in terms of standard deviation, so that our definition of F is their $(F)^2$.

In standard CCDs, the read noise dominates the variance at very low signal levels. This is not true for EMCCDs operating at high gain, as inspection of Equation (8) shows. Indeed, the main purpose of EMCCDs is to overcome read noise. The dominance of non-read noise sources at low light levels required us to develop specialized procedures to characterize EMCCD cameras.

1.4. Structure of Paper

The structure of this paper is as follows: Section 1 introduces the issues associated with using EMCCDs and defines terms. Section 2 describes the experimental set up and computational techniques used to characterize the devices. Section 3 summarizes the results of the characterization, which are interpreted in Section 4. Section 5 summarizes the paper and suggests directions for future research.

2. MATERIALS AND METHODS

2.1. Setup

All tests were performed using the basic setup shown in Figure 3. An integrating sphere coupled with a collimating telescope was equipped with a target wheel containing various spatial targets and bandpass filters. The camera under test was positioned so as to center the CCD in the clear aperture of the collimating telescope. A calibrated optical power meter was positioned between the camera and the collimating telescope using a magnetic kinematic mount to allow the removal and replacement of the power meter as needed (Figure 3). The CCD in the tested camera was kept at -30°C .

2.2. Data Acquisition

All data sets consisted of a series of multiple-frame images with nominally flat spatial profiles and associated dark frames. Band-limited light was used to illuminate the CCD, and the power meter was used to measure the irradiance for each exposure. The light level, exposure time, and gain setting for each image were recorded.

Since the optical power meter carried NIST-traceable calibration at the time of the experiment, the irradiance at the CCD could be calculated with an uncertainty of $\pm 2\%$. The power meter has a sensor area of 1 cm^2 and reports the total incident power in Watts, so the number of photons incident on each CCD pixel per frame is given by:

$$ph = (P \cdot t \cdot a) / (h \cdot c / \lambda) \quad (9)$$

P is the power meter reading, t is the exposure time, a is the area of a single pixel, and λ is the wavelength of light, c is the speed of light, and h is Planck's constant.

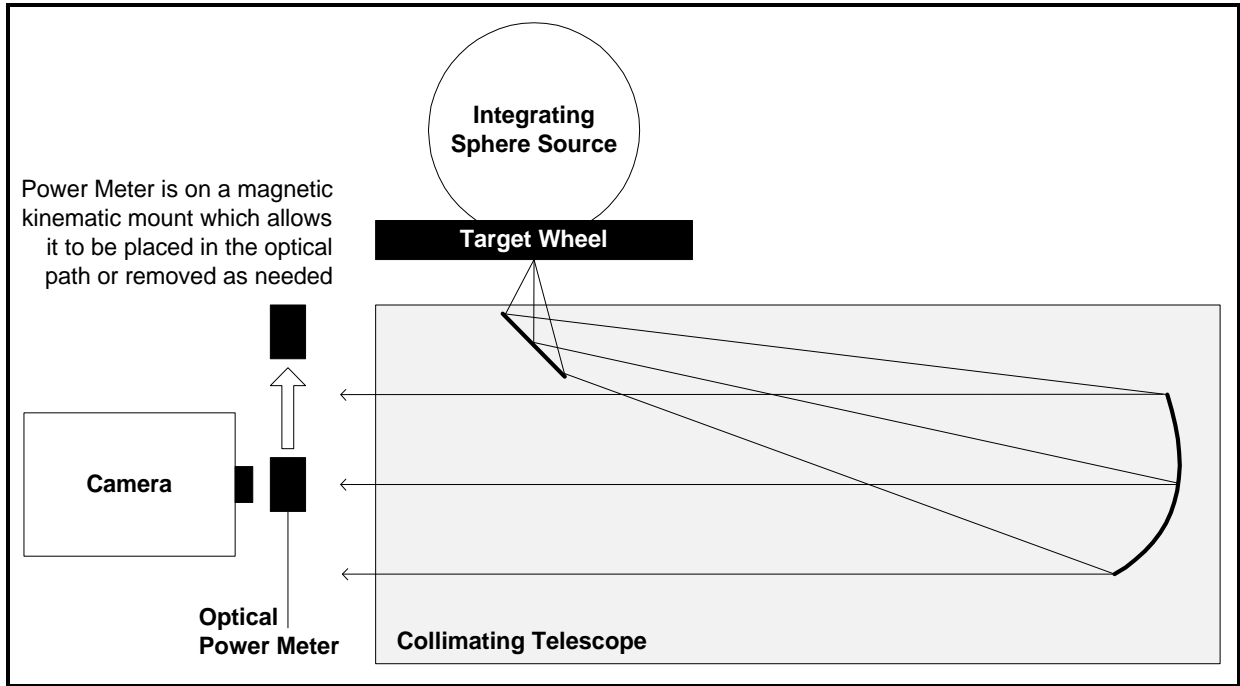


Figure 3. Basic laboratory setup for testing EMCCDs.

2.3. Photon Transfer Curve

For a standard CCD camera, the photon transfer curve (PTC) described by Janesick [2, Ch. 2] may be used to extract the read noise, pixel full well, and the video gain A in DN per electron. Janesick's PTC method relies on the assumption that the noise is additive, as in Equation (7). At low temperature, the dark noise is negligible, so that:

$$S_{Total, DN}^2 = S_{Read, DN}^2 + S_{Shot, DN}^2 + S_{Dark, DN}^2 + S_{FP, DN}^2 \quad (10)$$

The method also assumes that when flat images are differenced, the fixed pattern noise is removed and the remaining noise is comprised of read noise and shot noise alone²:

$$s_{DifferencedFrames,DN}^2 = s_{Read,DN}^2 + s_{Shot,DN}^2 + s_{Dark,DN}^2 \quad (11)$$

In the data analysis, the total noise, and the read, shot, and fixed pattern noises are plotted versus the average signal, S_{DN} . Read noise and pixel full well are read directly off the graph, and the video gain is found with Equation (12):

$$A = s_{Shot,DN}^2 / S_{DN} \quad (12)$$

The assumptions made in Equations (11) and (12) are sufficient when dealing with traditional CCD sensors. However the assumptions become invalid when additional noises are present in the system, so that the excess noise factor F exceeds unity, as is the case with EMCCDs. If the above method is used to analyze an EMCCD, F will be included in the shot noise term ($s_{Shot,DN}^2$) and the method of determining video gain, Equation (12), becomes invalid.

By turning off the electron multiplication, we can assume $M=1$ and essentially eliminate the effects of the additional gain stage, so that:

$$pe_{post}^- = pe_{pre}^- \quad (13)$$

$$s_{post,e-}^2 = s_{pre,pe-}^2 \quad (14)$$

In this case the EMCCD operates as a standard CCD and the video gain A can be determined with the traditional Janesick method. We then take A to be constant as M increases.

2.4. Quantum Efficiency

The quantum efficiency for a given wavelength is the ratio of the signal photo-electrons to incoming photons, and was determined using the setup shown in Figure 3, which allows us to calculate the number of incoming photons for each exposure. Since we now know the video gain from the photon transfer curve described above, we can combine equations (2), (3), and (4) to arrive at the following expression for quantum efficiency:

$$QE_I = \frac{S_{DN}}{G \cdot ph} \xrightarrow{M \rightarrow 1} \frac{S_{DN}}{A \cdot ph} \quad (15)$$

Equation (15) defines QE using parameters that can be easily tested in a lab environment by comparing the average signal generated from flat images of band-limited light with the known number of incoming photons. A QE curve generated this way is shown in Figure 4.

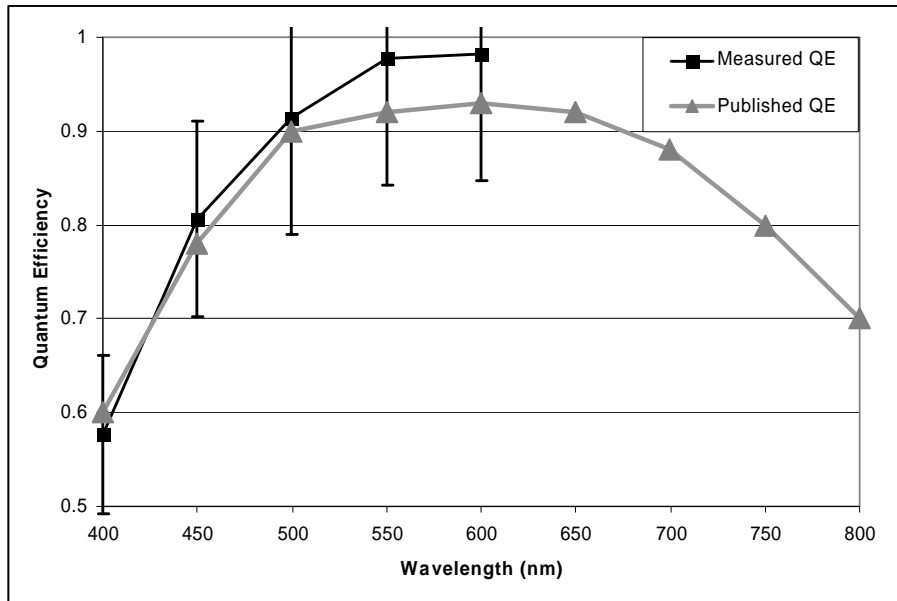


Figure 4. Quantum efficiency calculated using Equation (15) versus published QE.

2.5. Photo-Response

The photo-response is a plot of average DN's for the frame versus mean incident photons. The slope of the curve is the absolute photo-response of the camera in units of DN's per incident photon. By combining equations (5) and (15) we arrive at the following testable definition of absolute photo-response:

$$R_1 = QE_1 \cdot M \cdot A = \frac{S_{DN}}{ph} \quad (16)$$

2.6. Noise Equivalent Contrast

The noise equivalent contrast is a plot of the noise/signal as a function of incoming photons.

$$NEC = \frac{1}{SNR_{Camera}} = \frac{S_{Total,DN}}{S_{DN}} \quad (17)$$

The NEC curve in **Figure 5** may be generated by combining the photon transfer curve and the photo-response. In evaluating marine remote-sensing systems, the NEC requirement is determined from the characteristics of the target being sought; some targets require NEC on the order of 1% or less.

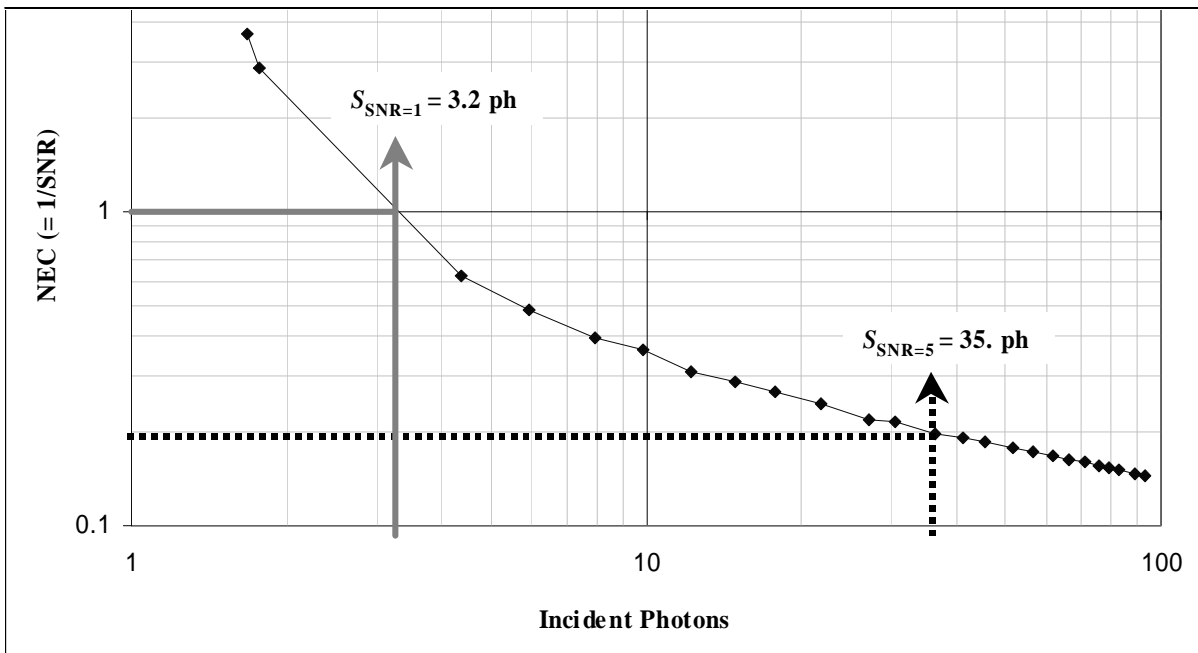


Figure 5. NEC versus incident photons, showing signals for two SNRs of interest.

2.7. Noise Factor Estimation

The definition of noise factor for the EMCCD gain process is:

$$F = \frac{S_{post,e-}^2}{M \cdot S_{pre,pe-}^2} \quad (18)$$

In the course of evaluating EMCCD cameras, we developed a methodology for estimating F using equipment readily available and methods that are applicable to unmodified off-the-shelf cameras.

If we assume that the read noise is uncorrelated with the output of the EMCCD, then:

$$S_{DifferencedFrames,DN}^2 = A^2 S_{post,e-}^2 + S_{Read,DN}^2 \quad (19)$$

Then:

$$s_{post,e-}^2 = (s_{DifferencedFrames,DN}^2 - s_{Read,DN}^2) / A^2 \quad (20)$$

Substituting (19) and (20) into (18) yields:

$$F = \frac{s_{post,e-}^2}{M^2 s_{pre,pe-}^2} = \frac{(s_{DifferencedFrames,DN}^2 - s_{Read,DN}^2) / A^2}{M^2 s_{pre,pe-}^2} = \frac{(s_{DifferencedFrames,DN}^2 - s_{Read,DN}^2)}{G^2 s_{pre,pe-}^2} \quad (21)$$

From Poisson statistics:

$$s_{pre,pe-}^2 = p e_{pre}^- \quad (22)$$

Then:

$$F = \frac{(s_{DifferencedFrames,DN}^2 - s_{Read,DN}^2)}{G^2 p e_{pre}^-} = \frac{(s_{DifferencedFrames,DN}^2 - s_{Read,DN}^2)}{G \cdot S_{DN}} \quad (23)$$

Thus, F is now expressed in terms of easily measurable quantities. Operationally, we would estimate the read noise as:

$$s_{Read,DN}^2 = s_{DifferencedFrames,DN}^2 (Exposure = 0, Light = 0) \quad (24)$$

Equation (23) is the basis of the method for estimating the noise factor from the PTC: for signals much greater than the noise floor, the slope of equation (23) equals F . Figure 6 shows examples of results for different gains. In practice, we limited signals to less than 100,000 electrons so as to minimize the effects of the video gain non-linearity. In addition, we required the signal to be at least 30,000 electrons, to be sure of working well above the noise floor.

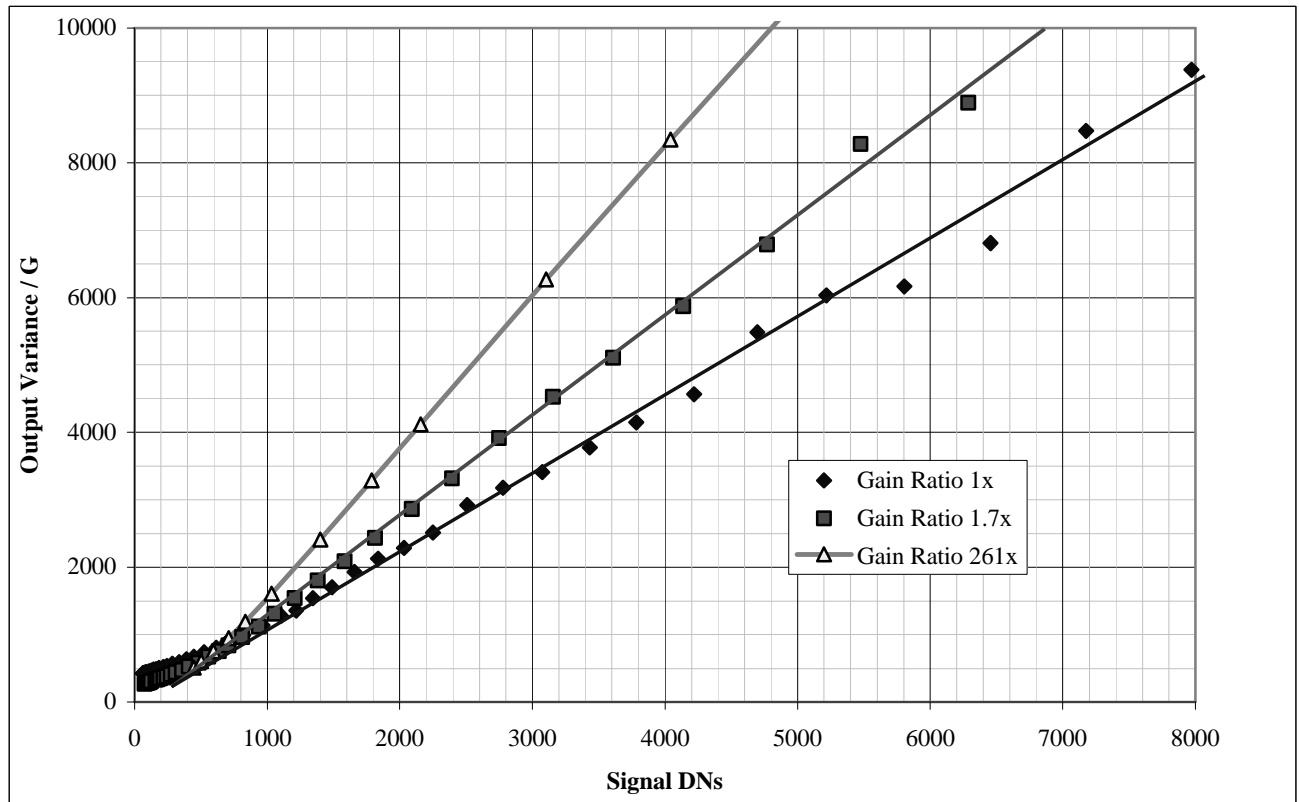


Figure 6. Noise factor estimation method. The slope of the portion well above the noise floor equals the noise factor F .

3. RESULTS

3.1. Photon Transfer Curves and Noise Factor Estimation

The PTC of an EMCCD operating with an EM gain ratio, $M = 1$, such as that shown in Figure 7, has exactly the same shape as the PTC of a standard CCD. Figure 8 shows the PTC of an EMCCD operating with an EMGR of 262x ($M = 262$). From the PTC, we derived slopes for use in the noise factor estimation procedure derived from Equation (23).

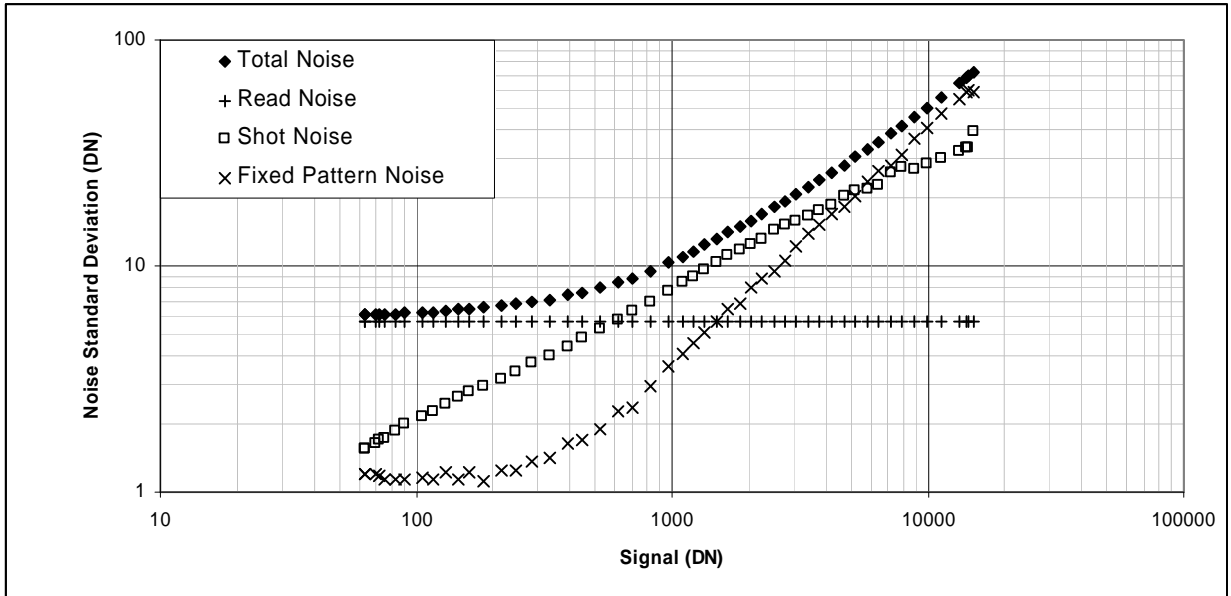


Figure 7. Photon transfer curve with $M=1$.

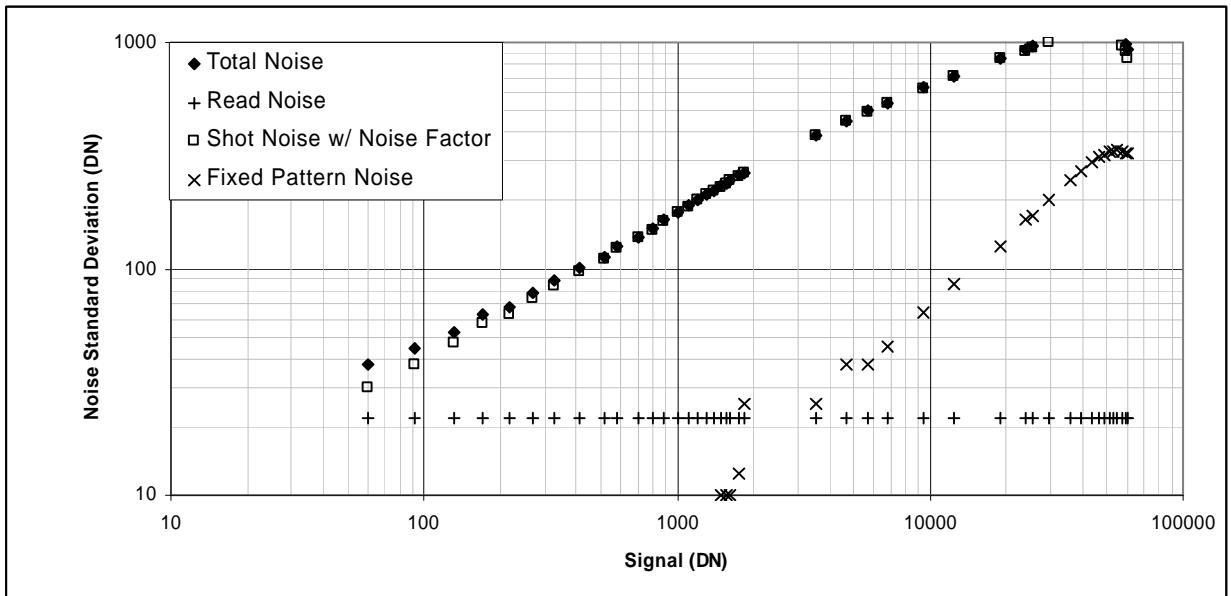


Figure 8. Photon transfer with $M = 262$, showing noise factor influence on slope.

The excess noise factor as a function of gain is shown in Figure 9. As the gain increases, the noise factor grows, saturating at $F=2$ at high gain. This is in accord with the results published in reference 1, which were obtained with a much more specialized procedure.

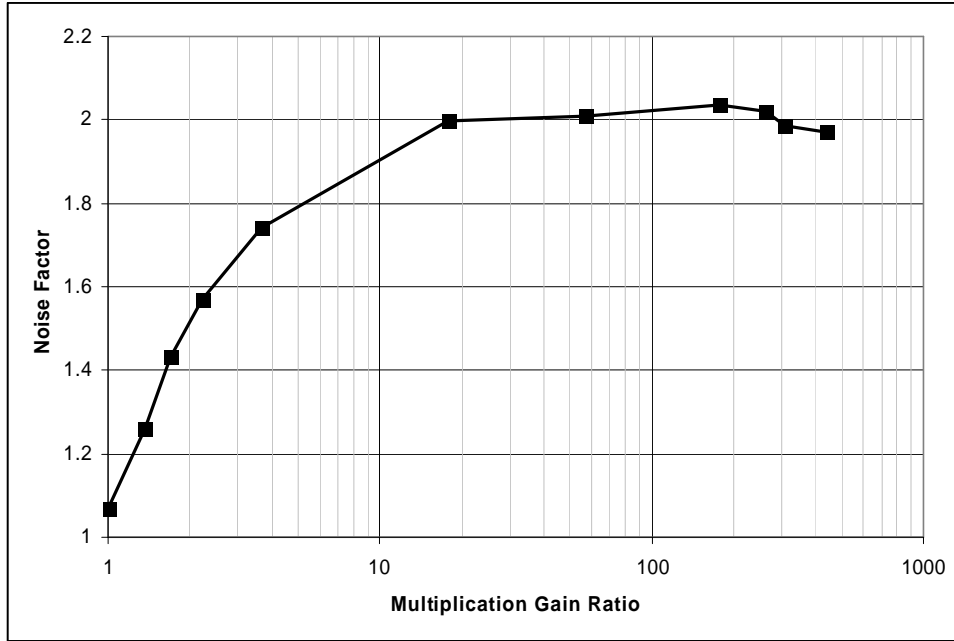


Figure 9. Excess noise factor versus electron multiplication gain.

3.2. Usable Signal Range and Dynamic Range

The dynamic range of a CCD imager is usually defined in terms of its full well capacity and read noise²:

$$DR = \frac{FW_{DN}}{S_{Read,DN}} \quad (25)$$

However, Equation (25) is misleading for devices with gain before the read stage. When electron-multiplication gain is present, Equation (25) yields a dynamic range which grows as M increases, regardless of shot noise:

$$DR = \frac{FW_{DN}}{S_{Read,DN}} \approx \frac{G \times FW_{pe}}{AS_{Read,e-}} \approx M \frac{FW_{pe}}{S_{Read,e-}} \quad (26)$$

Equation (26) implies dynamic ranges far in excess of what the device can actually produce because it doesn't account for sources of noise that dominate once the read noise has been rendered insignificant by the gain process. In our applications, we have found USR to be a more useful metric of optical system performance, especially with EMCCD-based imagers:

$$USR_{SNR} = \frac{FW_{DN}}{S_{SNR}} \quad (27)$$

S_{SNR} is the signal for which the SNR equals some application-specific threshold value. USR_{SNR} is a quantity akin to the *real dynamic range* cited by other researchers³ (we use the term useable signal range to avoid confusion). Like the various SNRs, USR_{SNR} will typically depend on system parameters, such as temperature and gain.

S_{SNR} should be determined at an operationally important SNR. The minimum SNR that would normally make sense is $SNR=1$. Thus, S_j yields the maximum USR, USR_j . Using (8) and the condition $SNR = 1$:

$$1 = SNR^2 = \frac{S_{DN}^2}{\mathbf{s}_{Total, DN}^2} = \frac{G^2 (pe_{pre, SNR=1}^-)^2}{A^2 \mathbf{s}_{Read, e-}^2 + G^2 F \cdot pe_{pre, SNR=1}^- + G^2 \mathbf{a}_{fp, DN} \cdot pe_{pre, SNR=1}^-^2 + \frac{1}{12}} \quad (28)$$

This is achieved at a signal level of:

$$pe_{pre, SNR=1}^- \approx \frac{1}{2(1-\mathbf{a}_{fp, DN})} \left[F \pm \sqrt{F^2 + 4(1-\mathbf{a}_{fp, DN}) \left[\frac{1}{G^2} \left(A^2 \mathbf{s}_{Read, pe-}^2 + \frac{1}{12} \right) + F pe_{Dark, pre}^- \right]} \right] \quad (29)$$

If the fixed-pattern noise is neglected, and if the device is cold enough for the dark noise to be negligible, Equation (29) reduces to:

$$pe_{pre, SNR=1}^- \approx \frac{1}{2} F + \sqrt{\left(\frac{1}{2} F\right)^2 + \frac{\mathbf{s}_{Read, pe-}^2}{M^2} + \frac{1}{12 G^2}} \quad (30)$$

The useable signal range is then approximated:

$$USR_1 = \frac{FW_{DN}}{S_{SNR=1}} \approx \frac{FW_{e-}}{\frac{1}{2} F + \sqrt{\left(\frac{1}{2} F\right)^2 + \frac{1}{M^2} \left[\mathbf{s}_{Read, pe-}^2 + \frac{1}{12 A^2} \right]}} \quad (31)$$

Unlike dynamic range, the USR is well behaved as the EMCCD gain M increases,

$$USR_1|_{M \rightarrow \infty} = \frac{FW_{e-}}{F} \quad (32)$$

That is, the usable signal range is limited by the capacity of the device and the excess noise factor. This limitation also applies to the video gain full well. That is why our USR and DR curves all go down for high EMG gains. Ideally, we would want to keep tuning the video gain in accordance with the EMG gain to maximize the USR.

In the other extreme, as the gain M is turned off, USR reduces to the normal definition of dynamic range:

$$USR|_{M \rightarrow 1} = \frac{FW_{e-}}{\frac{1}{2} + \sqrt{\frac{1}{4} + \mathbf{s}_{Read, pe-}^2 + 1/(12 A^2)}} \approx \frac{FW_{e-}}{\mathbf{s}_{Read, pe-}} = DR|_{M \rightarrow 1} \quad (33)$$

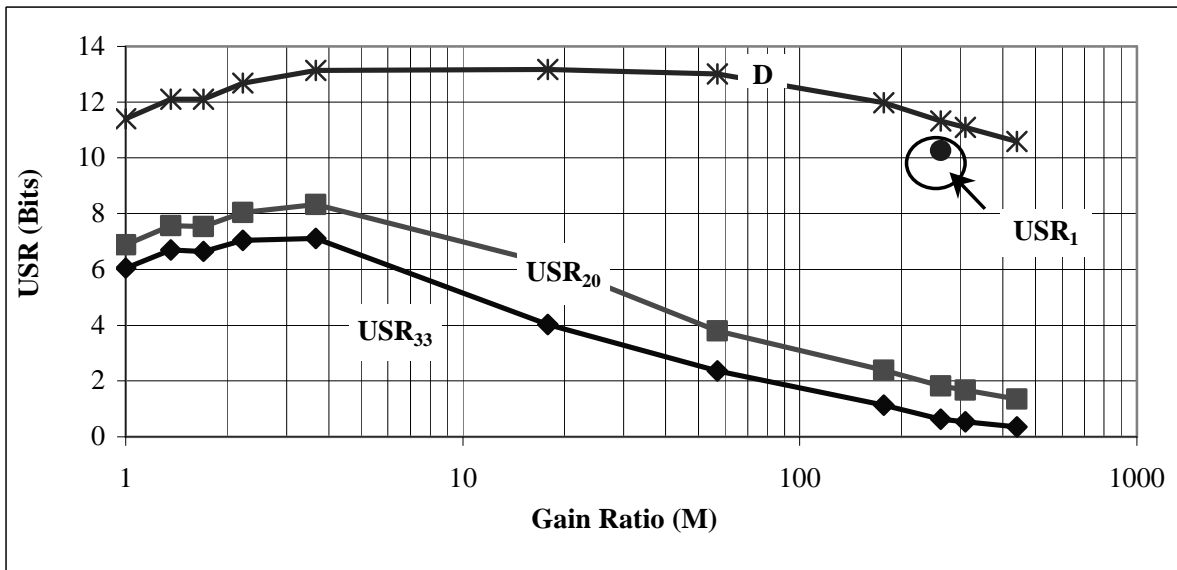


Figure 10. Dynamic range and USR for various SNR levels using the Cascade camera.

Several applications we have investigated require high SNR per pixel (low NEC), which reduces the USR. This is particularly true when discrimination of low-contrast image features is desired. The lower the feature contrast, the higher the required per-pixel SNR. Figure 10 shows USR_{33} , USR_{20} , USR_1 , and dynamic range computed from measurements of an EMCCD camera for various gain settings. A single measurement at very low light levels and a gain of 262 yielded the point labeled USR_I , which is almost exactly a factor of 2 below the corresponding dynamic range. This is in agreement with Equation (32), which predicted that the dynamic range should exceed USR_I by a factor of F at high gain.

4. DISCUSSION

As Figure 10 shows, dynamic range may greatly overestimate the actual useable range of a passive imaging device, depending on the application. This is particularly true for gain devices with a significant excess noise factor F : the useable range is automatically reduced by a factor of at least $1/F$. In practice, the useable range may be much less.

The good news is that the EMCCDs, operated under real-world test conditions, seem to have predictable excess noise factors of around 2. The use of gain to reduce the effects of read noise more than offsets the excess noise factor.

To date, our tests have focused on cold (-30°C) focal planes. In some applications, heat may be an issue. We plan to carry out tests to investigate possible temperature dependence of USR and F in the future.

5. CONCLUSIONS

EMCCD technology is a significant advance over previous image-intensification methods because it allows a high signal range with a modest excess noise factor. EMCCD technology effectively reduces the read noise by orders of magnitude so that read noise no longer determines the signal floor. Consequently, the dynamic range, as traditionally defined via Equation (25), can yield nonsensical results. To characterize EMCCDs, we have developed a new figure of merit, USR_{SNR} , and applied it to the characterization of EMCCD cameras. We determined that the dynamic range greatly overestimates the actual useable range, and plan to use USR to set performance requirements for future systems.

In the course of our characterizations, we confirmed that the EMCCDs are characterized by excess noise factors of approximately 2, which is consistent with published data. Our characterization, as summarized in Equation (23), relies on quantities that can be readily measured with standard cameras and optical laboratory equipment. Thus, the results presented in Figure 9 are applicable to the real-world performance of EMCCD cameras.

ACKNOWLEDGMENTS

The authors would like to thank Ulf Gustafsson of Science and Technology International (777 Bishop Street Suite 3100, Honolulu, HI, 96813). We also thank Dr. Doug Todoroff (Office of Naval Research) and Mr. Ned Witherspoon (Naval Surface Warfare Center) for their review and comments on this manuscript.

REFERENCES

¹ Mark Stanford Robbins and Benjamin James Hadwen, "The noise performance of electron multiplying charge-coupled devices", *IEEE Trans. Electron Devices*, **Vol. 50**, pages 1227-1232, 2003. Note that our F is Robbins's F^2 .

² James R. Janesick, *Scientific Charge-Coupled Devices*, Chapter 2, SPIE, Bellingham, WA, 2001.

³ Gerald C. Holst, *Holst's Practical Guide to Electro-Optical Systems*, p. 105, JCD Publishing, Winter Park, FL (2003).